ELSEVIER

Polymer 41 (2000) 7241–7253

polymer

"Multiple" nucleation of the (010) contact face of isotactic polypropylene, α phase

C. Mathieu, A. Thierry, J.C. Wittmann, B. Lotz*

Institut Charles Sadron (CNRS-ULP), 6, rue Boussingault, 67083 Strasbourg, France

Received 22 December 1999; accepted 12 January 2000

Abstract

Crystallization of isotactic polypropylene in its α modification (αiPP) can be initiated by a variety of nucleating agents. One of its (010) crystallographic planes is made of a highly symmetrical, lozenge shaped array of methyl groups. So far, this plane was known to interact only with substrates (benzoic acid and its salts, but also polyethylene through its bc contact face, and polyamides) with a ≈ 5 Å periodicity which matches a similar ≈ 5 Å periodicity normal to the *short diagonal* of the lozenge. In the present investigation, this same lozenge-shaped contact face is shown to interact with nucleating agents with periodicities of ≈ 4.2 and ≈ 6.6 Å which match periodicities normal to its *long diagonal* and to its *cell edges*, respectively. *Three* families of nucleating agents with very different periodicities can therefore interact with the *same* αiPP contact plane.

Keywords: Isotactic polypropylene; Crystal structure; Enhanced nucleation

1. Introduction

Physical interactions of epitaxial nature have been suspected early on to be the most likely interactions between non-reactive polymers (e.g. polyolefins) and their "nucleating agents", i.e. various low molecular weight organic materials or salts, or other polymers, which promote their "heterogeneous" nucleation [1]. However, a major concern about the applicability of epitaxial interactions has always been the observation that chemically and structurally highly diverse substrates can act as nucleating agents for any given polymer.

The role of epitaxial interactions has received strong support from a range of structural investigations, notably on polyethylene (PE) [2,3]. In spite of its "simple" molecular architecture (trans-planar chain conformation), PE crystallizes in two crystal modifications: stable orthorhombic and metastable monoclinic modifications. Electron diffraction investigations, often on substrate-PE bilayers, have demonstrated that the crystal planes of the orthorhombic or monoclinic modification of PE in which the inter-chain distance best matches the substrate periodicity become contact planes in the epitaxial relationship [3]. On this simple criterion of dimensional and structural matching of linear gratings, six different contact faces (three for each PE crystal modification) have been observed to act as contact planes [3]. Substrates active towards PE with periodicities ranging from ≈ 4 to ≈ 9.4 Å are diverse: alkali halides, organic acids and their salts, other low volatility organic materials (including a derivative of penicillin) [3] and other polymers (isotactic polypropylene and aliphatic polyamides) [4–7].

Isotactic polypropylene (iPP), the next member of the polyolefins family, also exists in four different crystal modifications with monoclinic (α), trigonal (β), orthorhombic (γ) and (presumably) hexagonal (smectic) cell geometries [8,9]. The chain conformation is always a 3-fold helix, which, in combination with the possible coexistence of right- and left-handed helices and often large unit-cell dimensions, makes analysis of interactions with nucleating agents less straightforward. However, several structural studies have shown that nucleating agents of iPP act also via epitaxial interactions. Specifically, these studies have shown that the α phase is induced by two families of substrates and the β phase by one family. For the α phase, a first family of substrates with a periodicity of ≈ 5 Å matches a 5.05 Å periodicity in the lateral $(010)_{\alpha iPP}$ face; this family includes benzoic acid and its salts, but also polyethylene and polyamides (this epitaxy applies also for the γ phase) [5]. The mode of action of the second family (which includes PTFE and other low MW organic hemiacids or salts of 4-chlorobenzoic acid) has been uncovered only recently: the epitaxy

* Corresponding author. Tel.: + 33-3-88-41-40-46; fax: + 33-3-88-41-40-99.

E-mail address: lotz@ics.u-strasbg.fr (B. Lotz).

0032-3861/00/$ - see front matter
PII: S0032-3861(00)00062-8

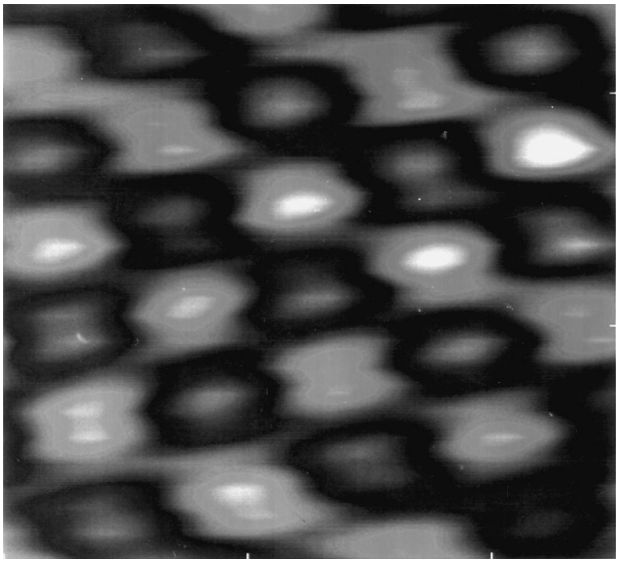

Fig. 1. Atomic Force Microscope image of the (010) contact plane of isotactic polypropylene (α phase) (αiPP) epitaxially crystallized onto benzoic acid. The dark spots represent methyl groups ≈6.5–6.6 Å apart (total imaged area: 2.5×2.5 nm^2). Note that AFM, which probes only the top surface of a lozenge-shaped array of methyl side chains, does not "feel" the chain axis direction, which is parallel to either one of the lozenge edges (this orientation can however be determined from the lamellar surface orientation, which can be visualized by AFM). Reproduced from Ref. [18] with permission.

rests on the matching of a ≈5 Å periodicity with equi-spaced rows of methyl groups in the (110) face of αiPP (this epitaxy *does not* apply for the γ phase) [10]. The β phase on the contrary is generated by nucleating agents (e.g. γ-quinacridone) [11] in which a ≈6.5 Å periodicity (and an orthogonal contact face geometry) matches the 6.5 Å chain axis periodicity (and the orthogonal geometry) of the (110) face of the trigonal, frustrated [12,13] unit-cell of βiPP [14].

The present investigation aims at extending these analyses to further classes of nucleating agents for iPP. Specifically, we concentrate on the ac face of αiPP [15], or the structurally equivalent ab face of γiPP [16,17] referred to above. Earlier studies have made it possible to analyze in considerable detail the structural and molecular characteristics of this contact face. In particular, AFM studies [18] have demonstrated that, out of two possible structurally different (010) contact faces, only the face with the lowest density of methyl groups is involved in epitaxy with e.g. benzoic acid. This same face is also involved in the homoepitaxy of γiPP [16,17] leading to a unit-cell with non-parallel chain axes, and by inference, in the homoepitaxy of αiPP onto itself [19,20], which results in the profuse lamellar branching characteristic of this phase.

As imaged by AFM (Fig. 1), the (010) contact face is a nearly "pure" array of lozenge shaped cells with methyl groups ≈6.5–6.6 Å apart at their corners. In this face, the helix axis (not seen by AFM) is parallel to either one of the two lozenge cell edges, depending on the hand of the imaged helices. So far, all nucleating agents which were found to interact with this face (such as e.g. benzoic acid) are characterized by periodicities near 5 Å, i.e. they "probe" and match the periodicity normal to the short diagonal of the lozenge (5.05 Å ($\bar{1}01$) interplanar distance). However, the intrinsic symmetry of the lozenge array suggests that two other families of nucleating agents may interact with this contact face: these are characterized by linear gratings of ≈4.2 Å and ≈6.6 Å periodicity, which would align parallel to the long diagonal of the lozenge and the lozenge edges, respectively (in the following, as an easy short-hand convention, chain axis repeats and inter-chain repeat distances are distinguished as 6.5 and 6.5 Å, respectively). The present report describes such nucleating agents and the diffraction data and analyses, which help characterize these further epitaxies. As such, it also illustrates the need to investigate polymer-nucleating agents interactions at the correct (local) scale before inferring (or rejecting) epitaxial interactions: a "global" analysis of the nucleating efficiency could hardly have predicted that three families of nucleating agents with widely different periodicities can interact with one and the same contact plane of αiPP.

2. Experimental

2.1. Samples

The sample of isotactic polypropylene mostly used in this investigation (with MW 315,000 and polydispersity ≈5.5) was provided by Elf-Atochem. It has already been used in several studies on enhanced nucleation [21–23] and in the investigation of iPP/PTFE interactions [10]. However, as frequently stated when dealing with investigations on epitaxial relationships, the molecular characteristics of the polymer (MW, polydispersity) are not of major importance, since crystallographic interactions at the unit-cell level are investigated.

Low MW organic materials used as nucleating substrates are of commercial origin, and are used without further purification.

2.2. Sample preparation

Following well-established procedures [24], the investigation of polymer/substrate epitaxy requires the preparation of thin layers of the polymer onto which a layer or a single crystal of the substrate is deposited. Electron diffraction patterns of the bi-constituent sandwich makes it possible to characterize the contact planes of the polymer and the substrate, as well as their relative orientations, i.e. provides all the information necessary to analyze the epitaxy. This complete information may not always be accessible, for various reasons: high vapor tension of the substrate, which does not allow its introduction in the vacuum of the microscope, difficulties in handling the bilayers during sample preparation or transfer to the electron microscope grid,

etc… Within these limits, two major preparation protocols have been used: (a) deposition or production of single crystals of the substrate onto a thin film of the polymer (cast on a glass cover-slide by evaporation from a dilute (0.5%) solution in e.g. *p*-xylene): this technique is used for alkali halides and salts or hemiacids of the organic acids; and (b) co-melting followed by crystallization of the polymer and the substrate between two glass cover slides, this procedure is applicable whenever the polymer is miscible in the solvent–substrate, and the latter crystallizes prior to the polymer. Its crystallization produces large, flake-like crystals onto which the polymer (by now rejected near the glass slides) crystallizes. Splitting of the two glass cover slides yields a thin polymer film which, after dissolution or sublimation of the substrate crystals, can be transferred to an E.M. grid. This technique is suitable for benzoic acid and the various substituted benzoic acids. Melting and recrystallization of iPP is often performed by using a Kofler bench, or in more controlled experiments by using a Mettler FP 80 computer-controlled hot stage. Dissolution of the substrates makes use of ethanol (for benzoic acid) or a 50/50 blend of acetone/heptane (good/poor solvent) for the substituted benzoic acids.

The thin films are shadowed (when desired), covered with a carbon film, floated on water and mounted on copper grids. Calibration of the diffraction patterns is made with the help of a thin layer of TlCl vaporized onto the polymer film.

2.3. Experimental techniques

Electron microscopic observations are made with a Philips CM12 microscope operated at 120 kV and equipped with a rotation-tilt specimen stage. The crystal structures and analyses of diffraction patterns are performed on a Silicon Graphics Indigo II workstation using the various packages available in the CERIUS 2 program for molecular modelization (Biosym-Molecular Simulations, Waltham, USA and Cambridge, UK).

3. Results

For the sake of completeness the main features of the epitaxy of isotactic polypropylene on benzoic acid (partly reproduced also in the course of this investigation) are recalled first, and complemented with other substrates with the same ≈ 5 Å periodicity. They may be considered as an introduction to the original results described in subsequent sections and in any case help "frame" the issues considered in this paper. At the onset however, it is necessary to recall (once again!) the crystal structure of αiPP, insisting on several features which are essential for the analysis of our data.

The crystal structure of αiPP is well established [8,15]. It has a monoclinic unit cell with parameters $a = 0.65$ nm, $b = 2.078$ nm, $c = 0.65$ nm, $\alpha = \gamma = 90°$, $\beta = 99.6°$, and space group either $P2_1/c$ or $C2c$, depending on relative chain orientation (clinicity) of the helices (the issue of clinicity will not be addressed in this work). As shown in Fig. 2a, the crystal structure is based on the packing of layers made of isochiral helices parallel to the ac plane, successive layers being made of helices that are both antichiral and oppositely oriented relative to the *b*-axis (one methyl group points alternately towards the $+b$ or $-b$ axis direction in successive layers). This complicated pattern of different helical hands and azimuthal settings generates four different ac faces, which differ either by the helical hand or the density of methyl groups in the (010) faces [9,18]. Two of these (010) faces are represented as seen in the $+b$ axis direction in Fig. 2b and c. Note the stagger of successive helices in the *c*-axis direction, which generates the monoclinic geometry of the unit-cell. In the present context, this stagger helps establish unambiguously the hand of the exposed helices (indicated with curved arrows). This holds true even for Fig. 2b, in which this hand is not apparent from the sole pattern of protruding methyl groups. As an easy rule of thumb, the helical path is parallel to the long diagonal of the lozenge when only one methyl group is exposed (as in this figure). In Fig. 2c on the opposite, exposition of two successive side chains (methyl groups) of the helix makes it an easy matter to determine the helical hand since the helical path is parallel to the short diagonal of the lozenge.

3.1. The short diagonal of $(010)_{\alpha iPP}$: substrates with a ≈ 5 Å periodicity

The crystal structure of benzoic acid is well known. The unit-cell is monoclinic with parameters $a = 5.51$ Å, $b = 5.157$ Å, $c = 21.973$ Å, $\alpha = \gamma = 90°$, $\beta = 97.1°$, space group $P2_1/c$ [25]. Benzoic acid crystallizes with prominent exposed ab faces in which the benzene rings are oriented nearly edge on. Epitaxy of iPP on benzoic acid (best revealed when using relatively low molecular weight iPP material, on account of the low melting temperature of benzoic acid: 122–123°C) rests on the matching of the 5.05 Å inter ⟨101⟩ row distance and the 5.16 Å *b*-axis periodicity of the acid: the *a*-axis of the benzoic acid is parallel to the short diagonal of the ac face of αiPP. This implication of the *diagonal* of the lozenge-shaped αiPP ac face in the epitaxial relationship has an interesting consequence: two helix axes orientations (which are parallel to the edges of the lozenge) are compatible with this condition; they are both tilted 50° away from this diagonal. As a result also, two populations of lamellae are generated, which are 80° apart (i.e. $180° - (2 \times 50°)$) (Fig. 2d). This relative orientation and organization of lamellae corresponds exactly to the structure of the so-called αiPP "quadrites" produced by solution crystallization and first investigated in detail by Khoury [19]. Indeed, the homoepitaxy at the root of the formation of these quadrites [20] (and of the lamellar branching observed also in bulk crystallization) is characterized by a similar parallelism of ⟨101⟩ directions in the two interacting lattices, and results in parallelism of a_1

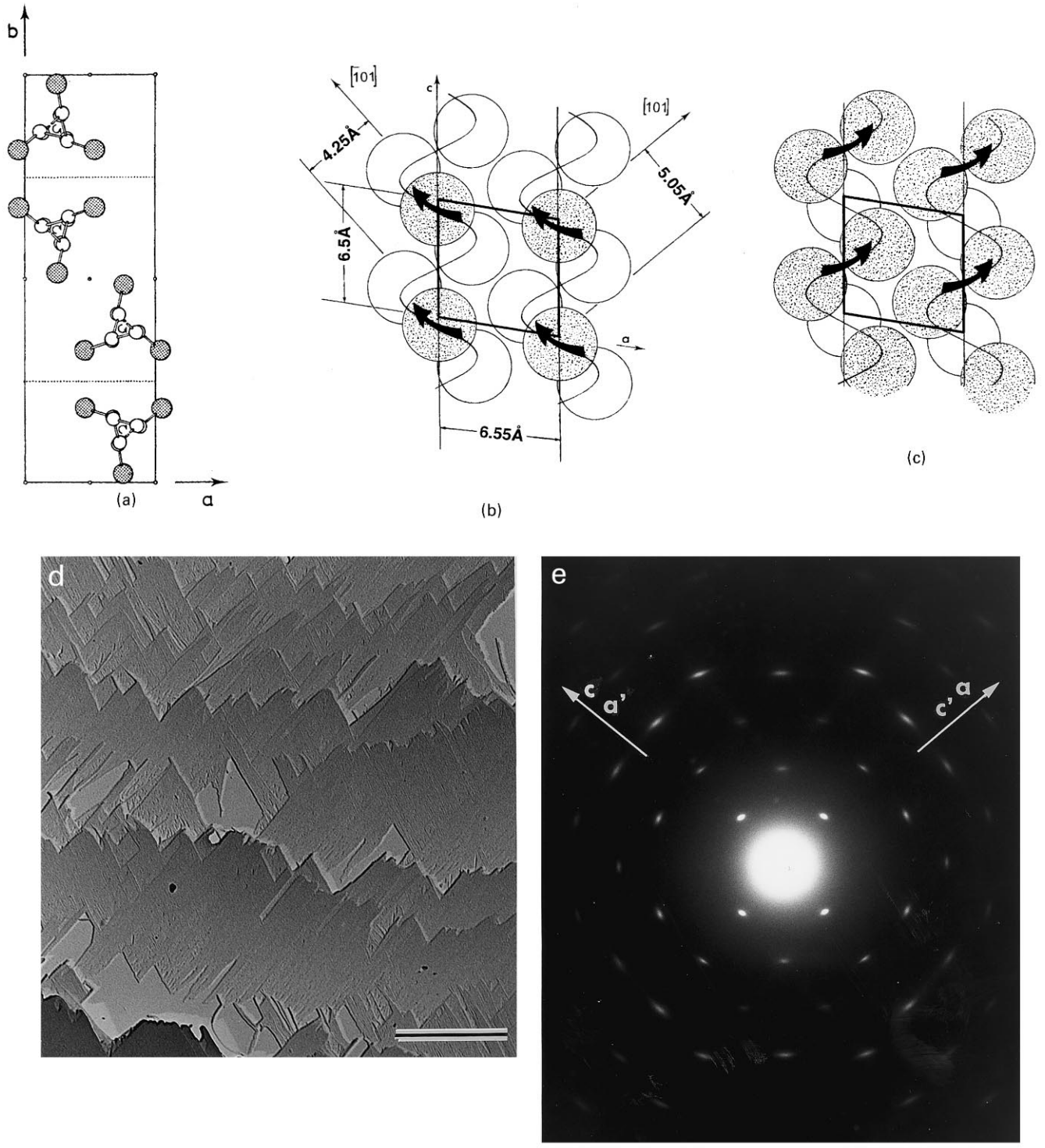

Fig. 2. (a) Unit-cell of αiPP seen in chain axis projection, with its alternation of layers made of right handed and left handed helices (all methyl side chains are shaded). (b) and (c) The pattern of methyl groups in the two structurally dissimilar (010) faces of αiPP with the helical hands indicated by curved arrows. Only the exposed methyl groups are shaded. Part (b) represents the first layer as seen along the *b*-axis direction (from the bottom of part (a)), part (c) the second layer. Note that when one or two methyl groups are exposed, the exposed helical path is parallel to the long or short diagonal of the lozenge, respectively. Mirror images of these schemes (with helical hands reversed, and dips of the *a*-axis to the left) would correspond to the (010) faces seen along the $-b$ axis direction (i.e. from the top of part (a)). Parts (b) and (c) share the same crystallographic planes and interplanar distances, only represented in part (b). The face in part (b) is considered as the contact face in the present work. (d) Epitaxially crystallized thin film of αiPP onto benzoic acid. Note the two lamellar orientations similar to those observed in solution or melt-grown quadrites. Transmission electron micrograph, Pt/C shadowing at $tg^{-1} = 1/3$, scale bar: 1 μm. (e) Electron diffraction pattern of a thin film as in part (d), with crystallographic axes indicated. Note parallelism of *a* and *c* axes in the two populations of lamellae of part (d).

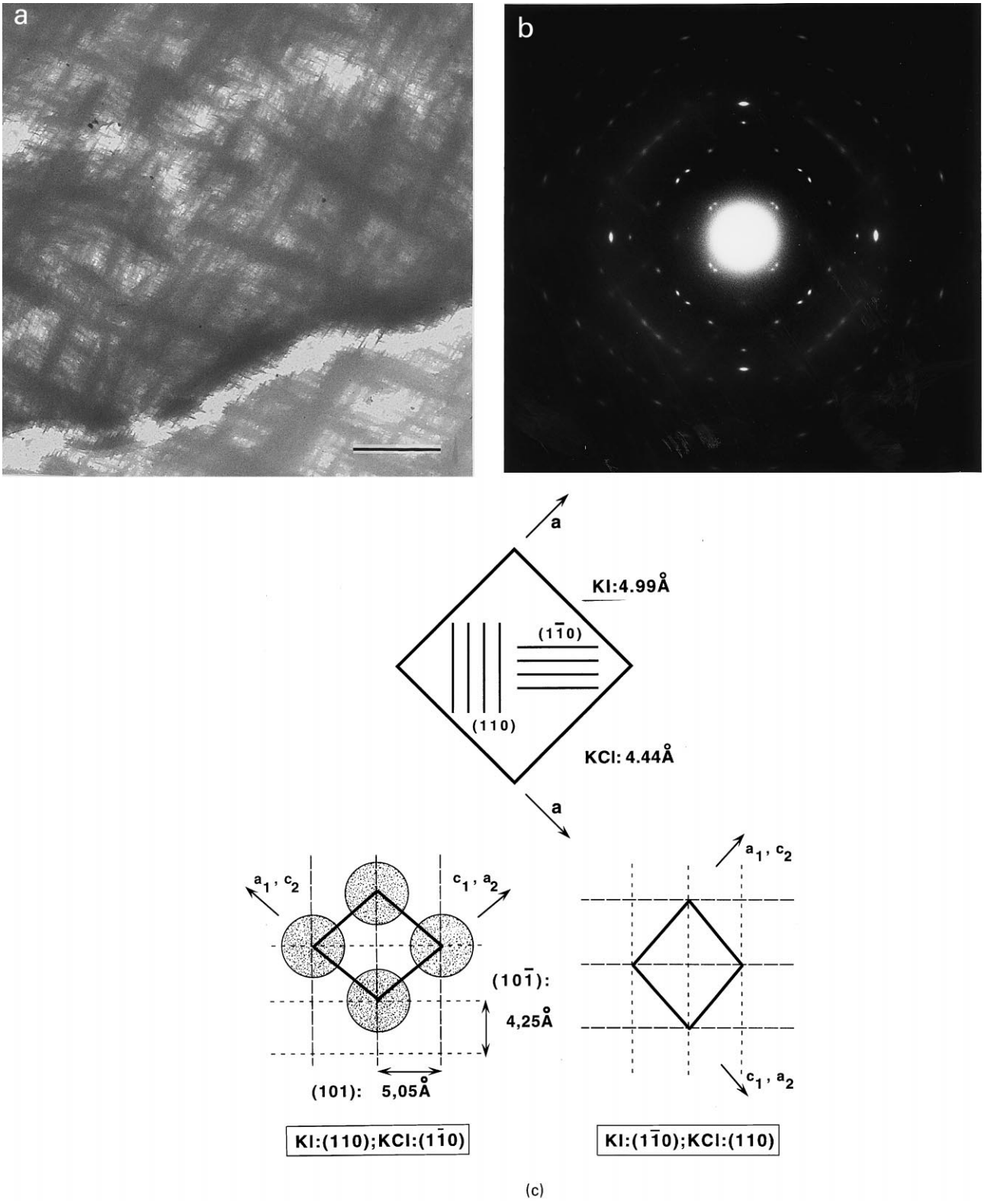

Fig. 3. (a) Lamellar morphology of a thin film of iPP vaporized, remelted and crystallized onto a (100) cleavage surface of KI. Bright field electron microscopy, unshadowed sample. Scale bar: 1 μm. (b) Electron diffraction pattern of a film as in part (a). Note that similar patterns have already been obtained by Ashida et al. [37] but have not been analyzed in terms of lattice matching with the substrate (part (c)). (c) Schematic representation of the epitaxy of the (010) contact face of αiPP onto the (100) cleavage face of KI and KCl. Note the similar, final orientation of the iPP contact face in spite of the fact that the epitaxies involve different periodicities. This similarity arises from the fact that diagonals are at right angles in both square (substrate) and lozenge (deposit).

and c_2 axes, and of a_2 and c_1 axes of the two lattices (and, as a further consequence, parallelism of $+b_1$ and $-b_2$) [20,26].

The diffraction pattern of αiPP films epitaxially crystallized on benzoic acid (which is similar to those of quadrites seen along the common *b*-axis [20]) is shown in Fig. 2e. It clearly corresponds to two 0*k*0 nets of αiPP rotated by $\approx 100°$ (the exact value is actually 99.6°, the β monoclinic angle of αiPP). Note that the six innermost reflections (110, 111) should not be visible, since they are of type *h*1*l*. However, these reflections are very strong, and located very near the *h*0*l* plane: they are therefore visible—and actually quite helpful in the analysis of the diffraction data. The lamellar morphology displayed in Fig. 2d and the diffraction pattern shown in Fig. 2e, and variations thereof, will be the basic features of the present investigation.

As developed in previous papers [18], the diffraction evidence presented in Fig. 2e does not help establish the exact topography of the contact face. Indeed, it does not (and actually cannot) help discriminate between the two structurally dissimilar (010) crystal planes that exist in αiPP (represented in Fig. 2b and c). This ambiguity can only be settled by probing the topography of the contact face by atomic force microscopy. The result of this AFM investigation [18] has been recalled in Fig. 1: the crystal plane with the lower density of methyl groups is the contact face. Basing our investigation on the assumption that this same contact face may be operative for other substrates (but this assumption has not been verified in the present work by parallel AFM investigations), we have undertaken to explore other potential nucleating agents for this same contact face, as described in subsequent sections.

Before moving on to these analyses, it may be worth pointing out the "flexibility" of the epitaxial relationship. Indeed, the $(010)_{\alpha iPP}$ contact plane observed for low molecular weight organic substrates such as benzoic acid is also obtained for a wide range of substrates which display the same ≈ 5 Å periodicity. Polymers such as polyethylene (bc face of PE, spacing 4.94 Å) and polyamides (ac face of e.g. PA11, spacing ≈ 4.8 Å) are also, under certain crystallization conditions, nucleating agents for αiPP [4,27–29]. These interactions can be used to produce bi- or multiply layers in which the chain axes of the iPP and PE or polyamides are, characteristically, 50° apart. Alkali halides [30] with a ≈ 5 Å periodicity are also suitable substrates: the epitaxy on potassium iodide (KI: cubic structure, $a = 7.05$ Å, (110) interplanar distance: 4.99 Å) is represented in Fig. 3a, and the corresponding diffraction pattern in Fig. 3b. This diffraction pattern appears at first sight rather complicated, but is simply the superposition at right angles (owing to the cubic symmetry of the substate) of two patterns such as shown in Fig. 2e. Fig. 3c details the epitaxial relationships between iPP and KI as well as with KCl (the latter to be examined later).

The search for substrates with different periodicities is not therefore restricted to organic materials but may extend to other types of substrates. However, the class of substituted aromatic acids is preferred for several reasons: easy availability, ease of handling, melting and crystallization in the suitable temperature range, good or fair compatibility with the polymer [24]. Most importantly in the context of the present work, substituted aromatic acids also offer an easy access to a wide range of periodicities, which are induced by various substituents, with in addition the possibility to position these substituents in ortho, meta or para positions.

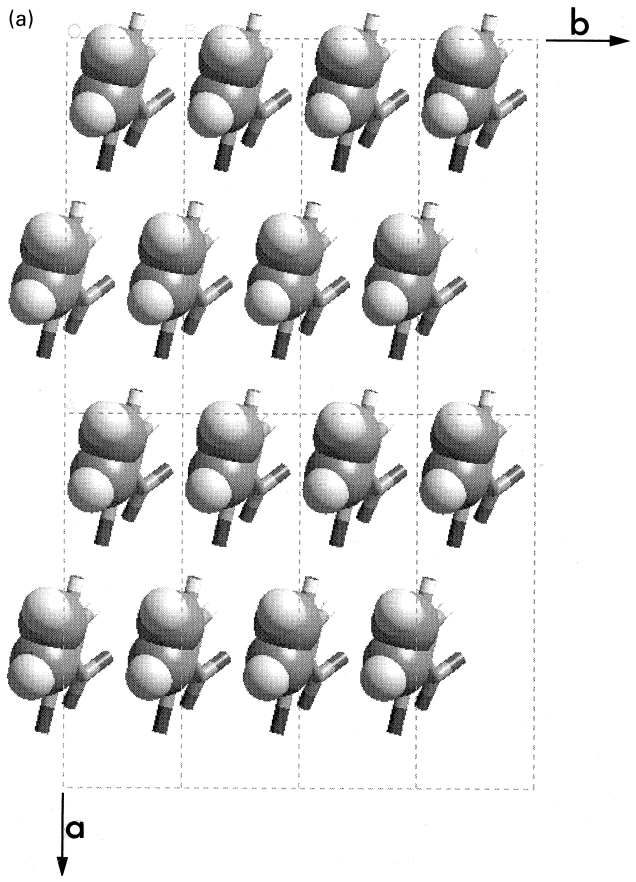

Fig. 4. (a) Molecular model of the ac contact plane of 2-bromobenzoic acid. The bromines, in ortho position, do not take part in the contact plane. Note the marked alignment of the benzene rings parallel to the (110) plane. (b) Lamellar morphology of an αiPP thin film epitaxially crystallized onto a 2-bromobenzoic acid crystal (the elongated crystal is horizontal). Note the tilt of the quadrite axis relative to the crystal edges, which helps discriminate between two possible epitaxial relationships. Transmission electron micrograph, Pt/C shadowing at $tg^{-1} = 1/3$, scale bar: 2 μm. (c) Schematic representation of αiPP onto the (001) face of 2BrBzAc. Parts (a)–(c) are in proper relative orientation. The substrate (100) planes and crystal edges are horizontal, (110) planes tilted at 18° to their normal. Orientation of the ac face of iPP based on matching of (110) planes in substrate and deposit. Lamellar orientation indicated supposes strict orthogonality of helical stems and fold surface, which is an oversimplification and explains the slight differences with orientations of lamellae observed in part (b). Favored growth of lamellae at 2 o'clock arises from likely preferential deposition of left-handed helices with axes parallel to c_1 with interacting *back* helical path (represented with a white arrow) parallel to substrate benzene rings in (110) planes.

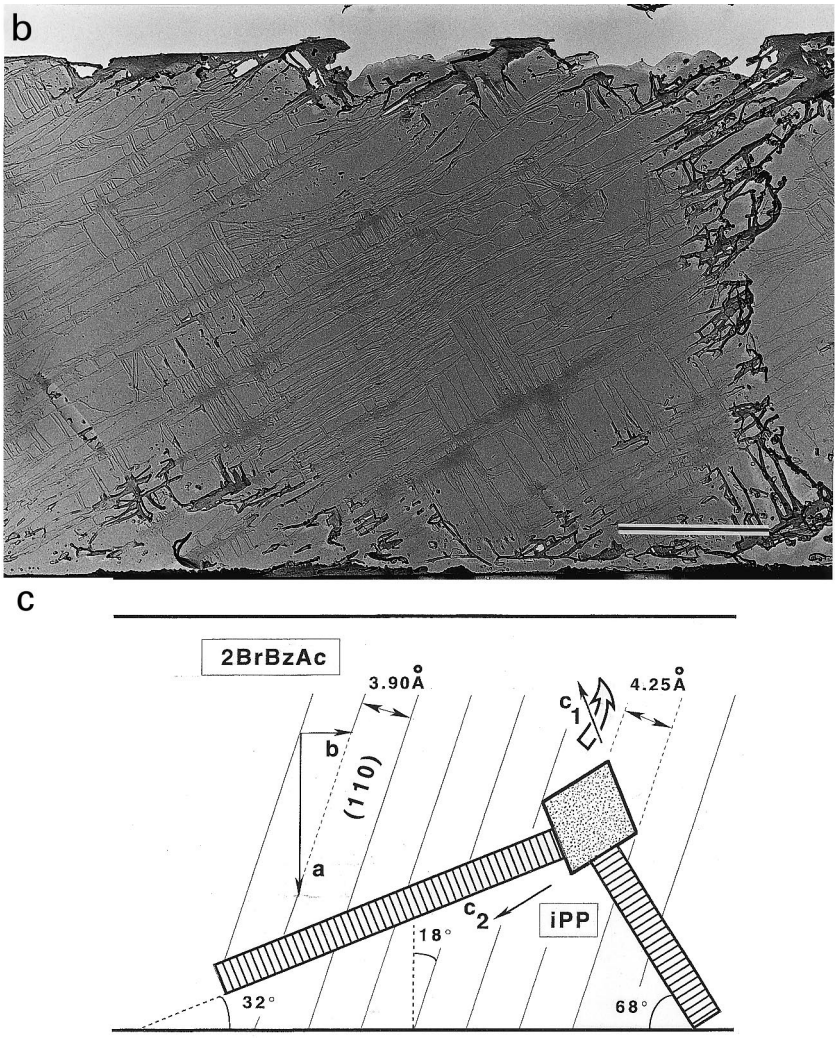

Fig. 4. (Continued).

Last but not least, the (often) low symmetry of the contact face facilitates analysis of the polymer/substrate interactions [24].

3.2. The long diagonal of $(010)_{\alpha iPP}$: substrates with a $\approx$ 4.25 Å periodicity

Both organic and alkali halides substrates have been found which interact with rows of methyl groups 4.25 Å apart in the (110) contact face of αiPP.

2-bromobenzoic acid (2BrBzAc) crystallizes in a monoclinic unit-cell with parameters $a = 14.82$ Å, $b = 4.10$ Å, $c = 25.90$ Å, $\beta = 118°$, space group C_2c [31]. As with all benzoic acid derivatives, the hydrogen bonded dimers form layers, with the apolar benzene ring end exposed in the contact face (Fig. 4a); the presence of a bulky bromine atom in ortho position of the acid moiety leads to a local overcrowding of the structure. The axis of the dimers is more tilted to the (001) contact surface than for benzoic acid, which leads to a fairly large distance between benzene rings: 7.41 Å, i.e. half the *a*-axis parameter. The bulkiness of the bromine atom also results in a larger than usual stacking of the benzene rings, thus the *b* parameter of 4.1 Å, which is close to, but on the short end of the 4.25 Å periodicity which is aimed for: the lattice mismatch amounts to −3.66%. Furthermore, successive layers along the *a*-axis are staggered by *b*/2, which leads to yet another prominent linear grating, this time along the (110) plane, with spacing 3.91 Å—definitely on the low edge for an epitaxial relationship, although the dimensional mismatch (−8.7%) would still be acceptable. Both values are therefore within "normal" limits for epitaxial relationships.

Epitaxy of iPP on 2BrBzAc yields an ac contact face, and displays the "quadrite-like" diffraction pattern with the characteristic two helix axis orientations (the pattern, not shown, is as in Fig. 2e). Since no lattice match other than that anticipated between the $\approx$ 4.2 Å periodicity of iPP in this ac plane can be figured out, we must conclude that the lattice match involves the "long" diagonal of the ac face of αiPP. No composite diffraction pattern of the polymer and

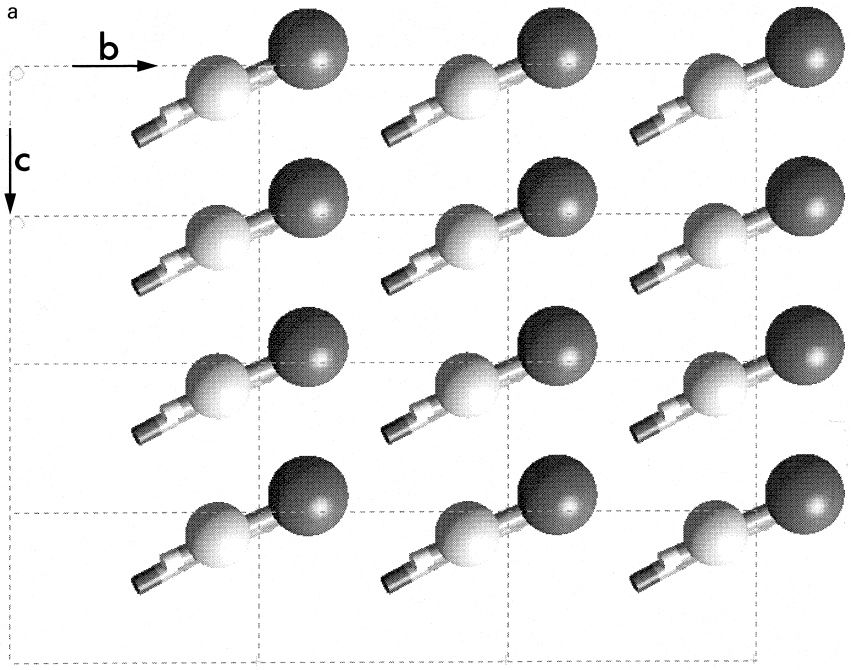

Fig. 5. (a) Molecular model of the bc contact face of 4-fluorobenzoic acid. The *b*-axis (6.38 Å periodicity) is horizontal, in correct relative orientation to the patterns displayed in parts (b) and (d). (b) Diffraction pattern of αiPP epitaxially crystallized onto the 4FBzAc bc contact face shown in part (a); (c) Analysis of the diffraction pattern shown in part (b): the latter is composed of two "quadrite-like" patterns (cf. Fig. 2e) which share one common *c*-axis direction (vertical); (d) "Asymmetric" diffraction pattern indicating a larger population of the quadrites shown on the right side of part (c). (e) "Selection" by dark field imaging of one out of the two populations of quadrites epitaxially crystallized onto 4FBzAc. A 111 diffraction spot (arrowed in part (b)) has been used. To help "read" the image, the two lamellar orientations are shown with white lines. Scale bar: 1 μm.

the substrate has been obtained, on account of the high vapor pressure of the acid. However, discrimination between the two potential substrate lattice planes ((100), 4.1 Å periodicity or (110), 3.91 Å periodicity) is possible by combining diffraction and morphology (orientation of the diffraction pattern relative to the substrate crystal outlines) or even on the basis of morphology alone, as outlined in Fig. 4b and c. In Fig. 4b, the *b*-axis of the 2BrBzAc crystal is horizontal (the stacking of benzene rings corresponds in most or all of these compounds to the fast growth). Two populations of iPP lamellae have crystallized on the substrate. They have different orientations relative to the long edges of the 2BrBzAc crystal (parallel to the *b*-axis). These two populations of lamellae are the components of quadrites; their different orientations indicates that the axis of the quadrite is tilted relative to the substrate *a* and *b* axes, which in turn indicates that the epitaxial match involves the (110) interplanar spacing of 2BrBzAc. The detailed structural analysis is indicated in Fig. 4c (the three parts of Fig. 4 are in correct relative orientation; mirror images would be obtained if the back face of the substrate were exposed). It sums up in a parallelism and matching of (110) planes of 2BrBzAc and iPP with interplanar distances of 3.9 and 4.25 Å, i.e. the iPP epitaxy favors structural matching (with the rows formed by the benzene rings in the (110) planes) in spite of a less favorable dimensional lattice match. The latter conclusion is further supported by a more thorough analysis of the morphology. In very thin iPP films as shown in Fig. 4b, lamellae oriented at 2 o'clock are much longer (have nucleated earlier and/or grown faster) than their counterparts oriented at 11 o'clock which very often abut on the 2 o'clock ones. This anisotropy reflects the structural asymmetry of the substrate contact plane, in spite of its geometric (orthogonal) symmetry (Fig. 4a). It suggests in turn that the epitaxial relationship is sensitive to the helical path of the depositing helix, and not only to the outermost lozenge shape pattern of methyl groups, as shown in Fig. 2b. If the contact plane is as shown in Fig. 2b, it is probable that the helical path illustrated in that figure is oriented parallel to the edges of the benzene planes of the substrate. Referring to Fig. 4c, this would mean that helices are deposited preferentially with their axis parallel to the c_1 orientation of the iPP unit-cell. This in turn indicates that deposition of left-handed helices (which interact through their back face with the substrate, in this representation) is favored for this orientation of the substrate unit-cell. Reciprocally of course, iPP epitaxy provides a molecular and morphological marker to determine the substrate *a* and *b* axes orientations.

Finally, in order to parallel the investigations reported above on the epitaxy on KI which involve the ≈ 5 Å periodicity, alkali halides with (110) interplanar distances near 4.25 Å were tested. NaBr would provide a near-perfect lattice match ((110) interplanar distance of 4.2 Å), but is highly hygroscopic. Epitaxies were obtained with KCl ((110) interplanar distance of 4.44 Å). The corresponding

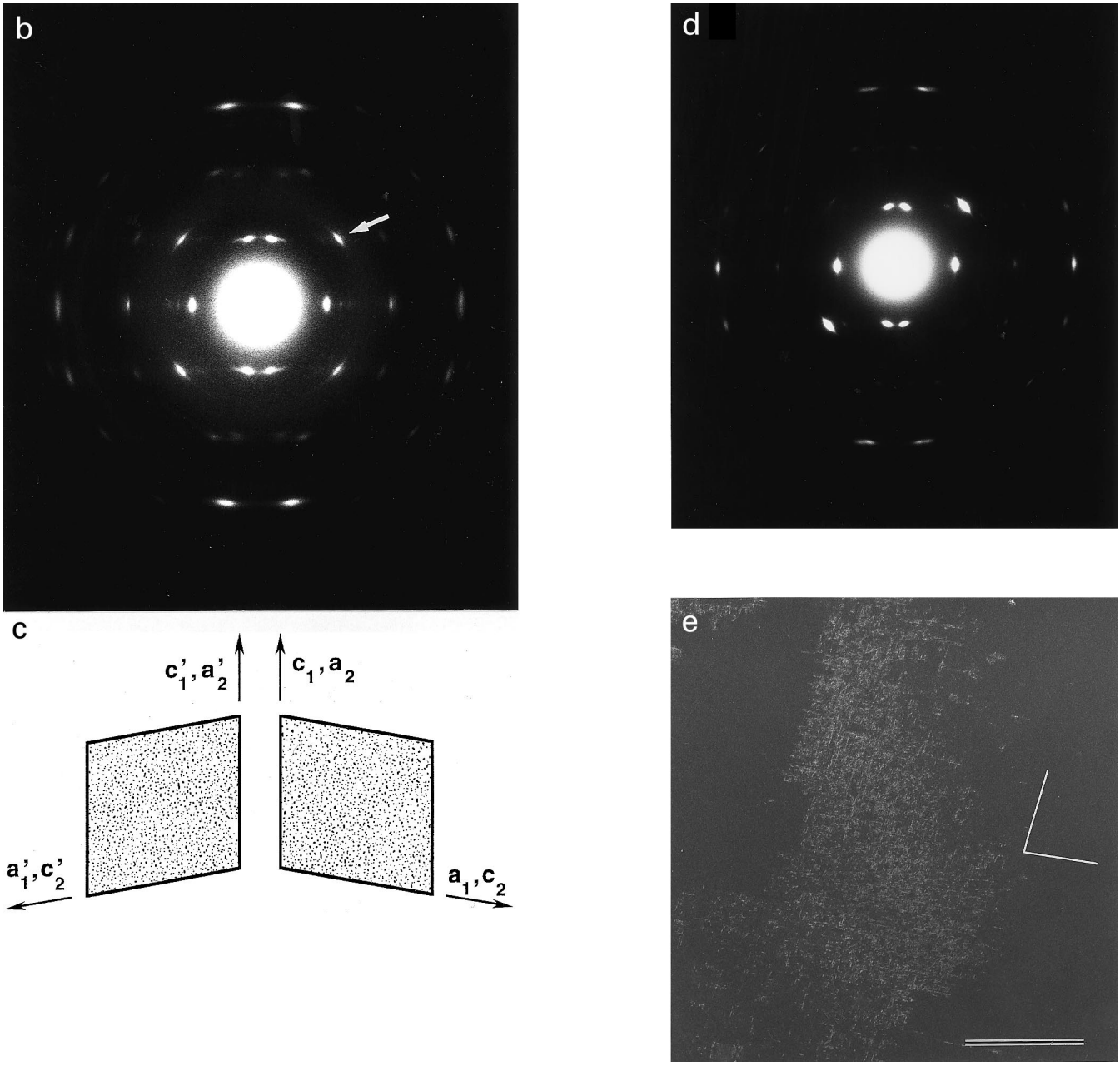

Fig. 5. (Continued).

diffraction patterns (not shown) are similar to those obtained on KI (Fig. 3a). Of course, the unit cell of iPP is oriented on KCl at 90° to that observed for KI, as illustrated in Fig. 3c. Since however two orientations at right angles to each other exist on the alkali halides, the final morphology is identical for the different substrates (with two sets of quadrites at right angles and with the same orientation) in spite of the fact that two different epitaxies (involving the 5.05 Å and the 4.25 Å αiPP periodicities) are at play.

Note that similar epitaxies were obtained on KBr ((110) interplanar distance of 4.65 Å). Since however this distance is within ±10% of both iPP 4.25 and 5.05 Å, ascribing the epitaxial relationship specifically to any of these two spacings is ambiguous. Note furthermore that the *a* parameter of KBr is 6.578 Å, which would provide the basis for a different type of epitaxy (as discussed now), but the diffraction data are inconsistent with this other possibility.

3.3. The cell edges of $(010)_{\alpha iPP}$: substrates with a ≈ 6.6 Å periodicity

Selection of an appropriate substrate to induce epitaxy with the cell edges of the ac faces is more constrained than for the ≈ 4.2 Å periodicity. Indeed, the periodicity to be matched is ≈ 6.5–6.6 Å, which is also the chain axis repeat distance of the 3-fold helix of iPP. Substrates with a

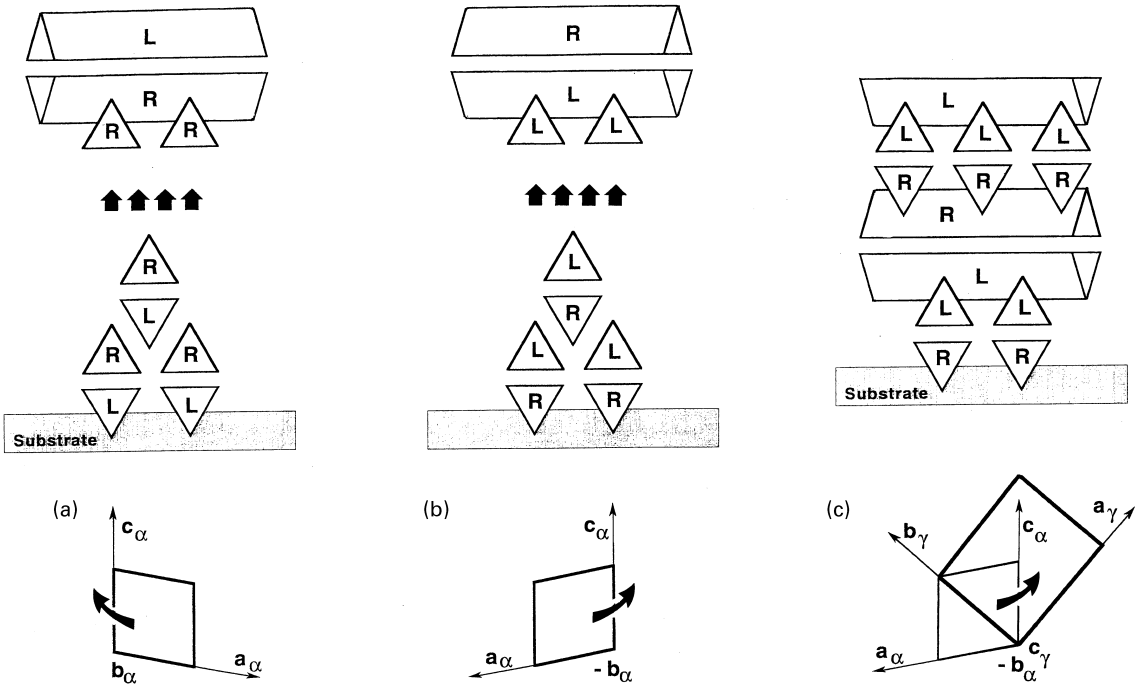

Fig. 6. Analysis of the helical hands of stems interacting with a substrate with 6.6 Å periodicity (cf. Fig. 5) and subsequent sequence of helical hands away from the substrate for different α phase *a*-axis orientations and crystal phases (α or γ). The cell projections (bottom of the figures) are as seen *through* the substrate, i.e. from the bottom of the upper part drawings. The two orientations of the α phase unit-cell correspond to contact faces made of helices of opposite hands (compare parts (a) and (b), helical hand of the first layer recalled by a curved arrow in the bottom parts). Lamellar branching after some growth (symbolized by the row of bold arrows) involves layers of hands opposite to the initial layer, and generate two different chain axis orientations (in both cases, parallel to the respective initial *a*-axis orientations). The possibility to generate either α or γ phases from the same substrate arises from the fact that the two layers deposited first are structurally equivalent for α or γ phases (compare parts (b) and (c)). Differenciation between α or γ phases becomes possible *only* from the third layer away from the substrate and thereafter (different helical hands and chain axis orientations of the helices).

6.5 Å periodicity are actually able to induce the β phase of iPP, and the epitaxy involves indeed the chain axis repeat distance. We are dealing here with a very "touchy" periodicity, since different phases (α or βiPP) may be generated with substrates that are geometrically and structurally very similar. For the βiPP epitaxy however, a rectangular geometry of the substrate unit-cell contact face, matching that of the (110) contact face appeared to be a favorable feature [14].

In the present investigation, we have used a family of substrates with a $\approx$ 6.6 Å periodicity, namely fluoro-substituted benzoic acids, either in position 2, 3 or 4. On account of the small difference in the van der Waals radii of fluorine and hydrogen atoms, the crystal structures of these acids differ only slightly. Only the epitaxy on 4-fluorobenzoic acid (4FlBzAc) is described.

4-fluorobenzoic acid (4FBzAc) crystallizes in a monoclinic unit-cell of parameters $a = 26.56$ Å, $b = 6.38$ Å, $c = 3.82$ Å, $\beta = 93.81°$, space group $P2_1/c$ [32]. (the *b*-axis parameters of 2- and 3-FlBzAc are 6.7 and 6.8 Å, respectively). The easy cleavage plane, and contact plane in the epitaxy, is the bc plane. The bc contact face is shown in Fig. 5a, and displays well-characterized rows 6.38 Å apart parallel to the *c*-axis. The plane of the benzene rings is aligned nearly parallel to the (011) planes, with an interplanar periodicity of 3.27 Å. Note that twice this distance (i.e. 6.54 Å) is also a potential match for the epitaxy we are looking for, but has not been observed.

A thin film of iPP epitaxially crystallized on 4FlBzAc yields a very characteristic diffraction pattern, shown in Fig. 5b. At first sight, it appears strikingly similar to a fiber pattern, with a population of so-called "*a*-axis orientation" chains (cross-hatched lamellae, appearing in the form of 110 reflections on the first layer line) in addition to the normal "*c*-axis orientation" (*c* chain axis parallel to the fiber axis, in this case vertical). However, this is not a fiber pattern. Indeed, only one hk0 reflection, namely 110 (and its second order) is located on the "equator": the prominent 130 and 040 reflections are missing. Also, the first layer line is less populated than in a normal fiber pattern. This pattern actually consists of two "quadrite-like" patterns as shown in Fig. 2e. The two patterns are in a very characteristic and revealing relative orientation: they share one common *c*-axis orientation; the two other *c*-axis orientations are tilted by the standard 100° to this common orientation, as in the above mentioned "*a* axis orientation". The analysis of the patterns is indicated in Fig. 5c. This relative orientation of quadrite-like patterns confirms the essential features of the epitaxy: the iPP contact face is the ac face, and *one* chain orientation is induced by the substrate, i.e. the lattice

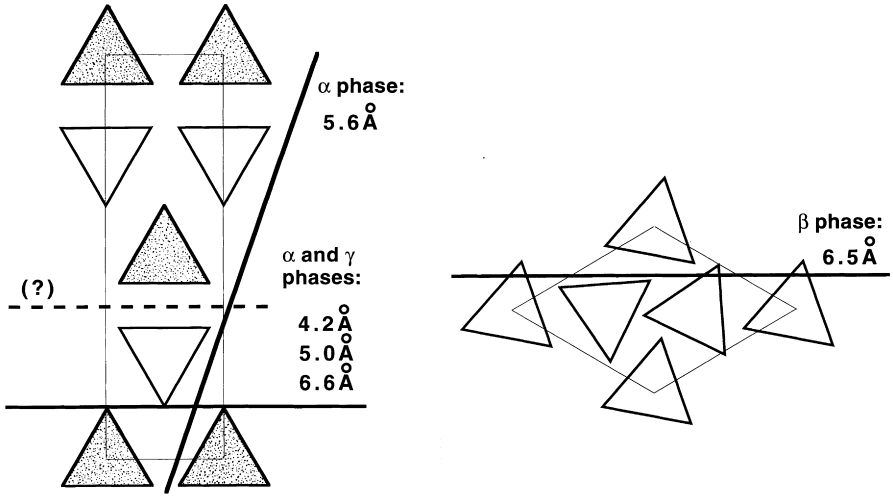

Fig. 7. Schematic summary of the epitaxies observed so far for the various crystal phases of isotactic polypropylene, and the corresponding lattice periodicities and specific crystal phase involved. Helices of opposite hands are shown shaded and unshaded, respectively. Setting angles of the β phase are as determined in Ref. [13]. For αiPP, the alternate (010) plane illustrated in Fig. 2c might be added to this diagram (broken line), but no evidence for its role as a contact plane has been obtained so far.

matching involves only the 6.6 Å interchain periodicity: in other words also, the epitaxy is able to differentiate the rows of methyl groups that correspond to the chain axis (as opposed to rows of methyl groups belonging to different helices) in spite of the apparent symmetry of the pattern of methyl groups in the contact plane (as illustrated in Fig. 1). However, depending on the hand of the helices which are deposited, the *a*-axis is tilted by 100° either to the right or to the left of this unique chain axis orientation. Further development and growth of iPP results in lamellar branching through homoepitaxy on the ac faces and induces a quadrite-like orientation, i.e. with "daughter" *c* (chain axis) orientations parallel to either one of the two initial *a*-axis orientations. Since two *a*-axis orientations exist in the initial epitaxially deposited layer, two superposed quadrite-like orientations are generated, which share one common *c*-axis orientation.

The above analysis is confirmed by occasional asymmetries of the diffraction pattern (Fig. 5d): in some areas of the epitaxially crystallized film, one of the quadrites may be more prominent than its counterpart, thus leading to an "asymmetric" diffraction pattern, which in turn confirms that the overall apparently "fibre-like" pattern is actually made of two distinct, "quadrite-like" components. A further illustration of this structural characteristic is provided by dark field imaging of the epitaxially crystallized film. The 111 reflections used for the imaging are located on the first "layer line" of the diffraction pattern: as shown in Fig. 5e, selecting one of them makes it possible to image the two sets of lamellae which build up one quadrite. Similar, symmetrical pictures (not shown) are obtained for the second set of quadrites using the other 111 reflection on the first layer line in the pattern of Fig. 5b.

Following a very simple reasoning developed in previous works [18,20], it is also possible to determine the hand (right or left) of helices involved in the initial epitaxy on 4FBzAc and in the development of subsequent lamellar branching (Fig. 6a and b). For this analysis, it suffices to recall that in ac faces of αiPP in which one methyl group is exposed, the underlying helical path is parallel to the long diagonal of the lozenge shaped ac face. With the assumption (confirmed by a wealth of experimental data [16–18]) that both the heteroepitaxy on 4FBzAc and the αiPP/αiPP homoepitaxy involve contact faces with one methyl group (cf. Fig. 1) and assuming further that the substrates are lying on top of the polymer film (i.e. looking at the latter from the viewpoint of the nucleating agent), the contact face in which the *a*-axis is tilted clockwise relative to the common chain axis orientation is made of left-handed helices. During subsequent growth away from the nucleating agent, homoepitaxy which generates the lamellar branching and the quadrite-like organization of lamellae involves facing layers made of right-handed helices. For the quadrite component for which the *a*-axis is rotated anticlockwise relative to the common chain axis orientation, the initial helices are right-handed, and subsequent lamellar branching involves facing layers made of left-handed helices. In other words, the diffraction pattern displayed in Fig. 5b, combined with the knowledge of the αiPP crystal structure makes it possible to define the hand and azimuthal setting of every helical stem in the epitaxially crystallized film (but not the clinicity, i.e. up- or down-orientation).

4. Discussion

Whereas the mode of action of nucleating agents has long been considered as a rather mysterious issue, development

of preparation protocols of thin bilayer films suitable for electron diffraction investigation (which helps assess nucleating agent/polymer crystallographic relationships) has underlined the prime role of physical interactions, i.e. of epitaxy. This issue has received considerable support in the case of polyethylene. As indicated in the introduction, adjustment of the lattice parameters of the substrate to the known interchain distances which exist in the orthorhombic and monoclinic phases of PE has made it possible to induce six different PE contact faces, three for each crystal modification [3].

The situation is more complex for isotactic polypropylene, due to the helical conformation of the chain and the coexistence of right- and left-handed helices in two out of the three polymorphs. However, substrates with periodicities of 5, 5.5 and 6.5 Å could be associated with various contact faces of either the α, β or γ phases of iPP. Up to now however, both in polyethylene and in isotactic polypropylene, any one substrate periodicity was known to induce only one contact face of the polymer.

The present investigation provides further and quite original support for epitaxial interactions in induced crystallization of polymers. Indeed, by taking advantage of the symmetry of the ac contact face of αiPP, substrates with three significantly different periodicities have been used (and in several cases predicted) to induce one and the same contact face of αiPP. In other words, the density of methyl groups in the contact face is constant, but is "felt" and "probed" differently depending on the substrate periodicities. Furthermore, since the epitaxies involve only the lateral ac face of αiPP, they are also valid for the γ phase: indeed, the two crystal structures are based on a common layer structure, although the α and γ phases are characterized by different sequences of helical chiralities of layers: for αiPP, an alternation of R(right) and L(left) layers (in short $(RL)_n$), and $(RRLL)_n$ for γiPP. The applicability of the nucleating agents to both α and γ phases stems from the fact that only one layer is initially involved in the epitaxial relationship. As shown in Fig. 6b and c, whether an α or a γ phase is formed can only be determined from the hand of helices in the third layer away from the substrate: if this hand is antichiral to that of the second layer helices, an α phase is generated, and helices are parallel; if it is isochiral, the chain axis lies at 80 or 100° to the second layer one, and a γ phase structure with non-parallel axes is created. The "flexibility" of substrates considered in this investigation towards the α and γ phase contrasts with the specificity of nucleating agents with a 5.5 Å periodicity (e.g. PTFE substrates) [10]: the latter apply *only* for the α phase but *not* for the γ phase. Indeed, these substrates match a linear grating of methyl groups 5.5 Å apart in the (110) plane of αiPP (which intersects the "building" layers common to α and γ phases). However, in the γ phase, such a plane would also intersect the chains, due to the unconventional tilt of the latter in that structure: the 5.5 Å periodicity of substrates can only induce α phase contact planes, which can be recognized as such at the onset. The various epitaxies analyzed for the different crystal phases of iPP, and the corresponding lattice distances are summarized in Fig. 7. Note that an orthogonal geometry of the contact plane (suggested as a possible criterion in an earlier investigation [10,14]) for the β phase has been abandoned: 4FBzAc has a periodicity close to 6.5 Å and an orthogonal contact plane, yet it induces the α phase rather than the β phase. Understanding the structural reasons for the "β phase specificity" of nucleating agents with $a \approx 6.5$–6.6 Å will require further analyses.

5. Conclusion

The set of experimental results presented in this paper adds to the considerable body of evidence which indicates that nucleating agents act primarily via epitaxial interactions with the polymers [24,33], at least when the latter are non-reactive. The analysis is rather straightforward for "simple" linear polymers (e.g. PE) in which mainly interchain periodicities are involved. Isotactic polypropylene is a more challenging polymer. Over 30 years ago, a kind of structural puzzle was uncovered when several nucleating agents were found to be active towards both PE and iPP [34], and that each of these polymers nucleates the other [35]. This puzzle was solved when it was realized that the $(\bar{1}01)$ interplanar distance in the ac face of αiPP has a 5 Å periodicity which matches the *b*-axis repeat distance of PE [36]. These planes are parallel to the bisector of the monoclinic β angle (≈ 100°), and the epitaxy, therefore, accounts also for the uncommon 50° angle between iPP and PE chain axes observed in extruded materials. The more recent elucidation of the β phase epitaxy on substrates such as γ-quinacridone (≈ 6.5 Å periodicity), and of the α phase on PTFE (5.5 Å periodicity), and the present observation that different directions (i.e. periodicities) in the same iPP contact plane may be activated are further steps in our understanding of iPP nucleation. In particular, the present study has shown that nucleation of iPP can be induced by substrates with periodicities on the much shorter side (≈ 4.2 Å or even, from our data, ≈ 3.9 Å) of the previously considered range (from ≈ 5 to ≈ 6.5 Å).

The present investigation demonstrates, probably for the first time in polymers, that different classes of nucleating agents (i.e. which act via different dimensional matchings) can interact with the same polymer contact face. The situation is exceptional, in that the (010) face of iPP, with its lozenge array of methyl groups, is highly symmetrical and "hides" to some extent its macromolecular character, since the helical path is rejected way behind the front methyl groups. This study further demonstrates that epitaxy cannot be postulated (or rejected!) on the sole basis of a priori arguments of unit-cell geometry or symmetry (of the substrate and/or polymer), but requires an intimate

knowledge of all facets of chain conformation and crystal structure of the partners involved in the epitaxial relationship.

With the elucidation of the nucleating activity of substrates which had resisted analysis up to now, a more complete picture of the epitaxy of iPP emerges, as summarized in Fig. 7. This figure shows that all the densely populated planes of iPP are involved in epitaxies, sometimes in uncommon ways (structurally identical planes for α and γ phases, different periodicities for the $(010)_\alpha$ plane). Efficient epitaxies involving less densely populated planes (e.g. (100) of βiPP) are presumably less likely, on account of the weaker interactions linked with the lower density of interactions. In other words, virtually all the planes susceptible to interact epitaxially with (efficient) nucleating agents for the various phases of iPP are displayed in Fig. 7. Present and future nucleating agents may vary widely in chemical and structural nature (various routes are indeed investigated in different laboratories), but they must fit in the above epitaxy frame, i.e. they must have a structural periodicity which matches one of those shown in Fig. 7.

References

[1] Sharples A. Introduction to polymer crystallization. London: Arnold, 1966 (p. 65–75).
[2] Wittmann JC, Lotz B. J Polym Sci, Polym Phys Ed 1981;19:1837.
[3] Wittmann JC, Lotz B. Polymer 1989;30:27.
[4] Lotz B, Wittmann JC. J Polym Sci, B: Polym Phys 1986;24:1559.
[5] Gross B, Petermann J. J Mater Sci 1984;19:105.
[6] Lee I-H, Schultz JM. J Mater Sci 1988;23:4237.
[7] Wittmann JC, Hodge AM, Lotz B. J Polym Sci, Polym Phys Ed 1983;21:2495.
[8] Bruckner S, Meille SV, Petraccone V, Pirozzi B. Prog Polym Sci 1991;16:361.
[9] Lotz B, Wittmann JC, Lovinger AJ. Polymer 1996;37:4979.
[10] Yan S, Katzenberg F, Petermann J, Yang D, Shen Y, Straupé C, Wittmann JC, Lotz B. Polymer 2000;41:2613.
[11] Leugering HJ. Makromol Chem 1967;109:204.
[12] Kopp S, Dorset DL, Lotz B. C R Acad Sci 1994;319:187.
[13] Dorset DL, McCourt MP, Kopp S, Schumacher M, Okihara T, Lotz B. Polymer 1998;39:6331.
[14] Stocker W, Schumacher M, Graff S, Thierry A, Wittmann JC, Lotz B. Macromolecules 1998;31:807.
[15] Natta G, Corradini P. Nuovo Cim Suppl 1960;15:40.
[16] Bruckner S, Meille SV. Nature 1989;340:455.
[17] Meille SV, Bruckner S, Porzio W. Macromolecules 1990;23:4114.
[18] Stocker W, Magonov SN, Cantow HJ, Wittmann JC, Lotz B. Macromolecules 1993;26:5915 (correction 27 (1994) 6690).
[19] Khoury FJ. Res Natl Bur Stand, Sect A 1966;70A:29.
[20] Lotz B, Wittmann JC. J Polym Sci, B: Polym Phys 1986;24:1541.
[21] Fillon B, Wittmann JC, Lotz B, Thierry A. J Polym Sci, B: Polym Phys 1993;31:1383.
[22] Fillon B, Lotz B, Thierry A, Wittmann JC. J Polym Sci, B: Polym Phys 1993;31:1395.
[23] Fillon B, Thierry A, Wittmann JC, Lotz B. J Polym Sci, B: Polym Phys 1993;31:1407.
[24] Wittmann JC, Lotz B. Prog Polym Sci 1990;15:909.
[25] Bruno G, Randaccio L. Acta Crystallogr C 1980;43:2239.
[26] Padden Jr. FJ, Keith HD. J Appl Phys 1966;37:4013.
[27] Lotz B, Wittmann JC. J Polym Sci, Part B: Polym Phys 1987;25:1079.
[28] Seth KK, Kempster CJE. J Polym Sci Polym Sci, Part C: Polym Symp 1977;58:297.
[29] Kojima M, Satake H. J Polym Sci Polym Phys Ed 1984;22:285.
[30] Koutsky JA, Walton AG, Baer E. J Polym Sci, Part B 1967;5:177.
[31] Ferguson G, Sinn GA. Acta Crystallogr 1962;15:346.
[32] Kubota M, Ohba S. Acta Crystallogr Sect B (Str Sci) 1992;48:849.
[33] Thierry A. In: Salamone JC, editor. Polymetric materials encyclopedia, vol. 3. Boca Raton, FL: CRC Press, 1996. p. 2167–79.
[34] Binsbergen FL. Polymer 1970;11:253.
[35] Last AGM. J Polym Sci 1959;39:543.
[36] Lotz B, Wittmann JC. Makromol Chem 1984;185:2043.
[37] Ashida M, Ueda Y, Watanabe T. J Polym Sci Polym Phys Ed 1978;16:179.